Overcritical Rotation of a Trapped Bose-Einstein Condensate

A. Recati,[1] F. Zambelli,[2] and S. Stringari[2]

[1]*International School of Advanced Studies, Via Beirut 2/4, I-34014 Trieste, Italy*

[2]*Dipartimento di Fisica, Università di Trento and Istituto Nazionale per la Fisica della Materia, I-38050 Povo, Italy*

(Received 6 July 2000)

The rotational motion of an interacting Bose-Einstein condensate confined by a harmonic trap is investigated by solving the hydrodynamic equations of superfluids, with the irrotationality constraint for the velocity field. We point out the occurrence of an overcritical branch where the system can rotate with angular velocity larger than the oscillator frequencies. We show that in the case of isotropic trapping the system exhibits a bifurcation from an axisymmetric to a triaxial configuration, as a consequence of the interatomic forces. The dynamical stability of the rotational motion with respect to the dipole and quadrupole oscillations is explicitly discussed.

DOI: 10.1103/PhysRevLett.86.377 PACS numbers: 03.75.Fi, 05.30.Jp, 32.80.Pj, 67.40.-w

An important peculiarity of harmonic trapping is the existence of a critical angular velocity, fixed by the oscillator frequencies, above which no system can rotate in conditions of thermal equilibrium. The main purpose of this paper is to show that a trapped Bose-Einstein condensate at very low temperature can rotate at angular velocities higher than the oscillator frequencies in a regime of dynamical equilibrium. The occurrence of overcritical rotations is a rather well-established feature in classical mechanics (see, for example, [1,2]) and is the result of the crucial role played by the Coriolis force. It is therefore interesting to understand the new features exhibited by rotating superfluids and in particular the role played by Bose-Einstein condensation. The rotational behavior of superfluids is, in fact, deeply influenced by the constraint of irrotationality which makes it impossible for such systems to rotate in a rigid way. Spectacular consequences of irrotationality are the quenching of the moment of inertia with respect to the rigid value and the occurrence of quantized vortices [3]. Both of these effects have been recently observed in dilute gases confined in harmonic traps [4–6].

We start our analysis by considering a dilute Bose gas interacting with repulsive forces at zero temperature. For large systems, where the Thomas-Fermi approximation applies, the equations of motion are well described by the so-called hydrodynamic theory of superfluids [7,8]. If the anisotropic harmonic confining potential rotates with angular velocity Ω it is convenient to write these equations in the corotating frame, where they take the form

$$\frac{\partial \rho}{\partial t} + \nabla[\rho(\mathbf{v} - \mathbf{\Omega} \times \mathbf{r})] = 0\,, \qquad (1)$$

$$\frac{\partial \mathbf{v}}{\partial t} + \nabla \cdot \left(\frac{v^2}{2} + \frac{V_{\rm ext}(\mathbf{r})}{M} + \frac{\mu_{\rm loc}(\rho)}{M} - \mathbf{v} \cdot (\mathbf{\Omega} \times \mathbf{r})\right) = 0\,. \qquad (2)$$

In the above equations $V_{\rm ext}(\mathbf{r}) = M(\omega_x^2 x^2 + \omega_y^2 y^2 + \omega_z^2 z^2)/2$ is the oscillator potential providing the external confinement, for which we will choose $\omega_x > \omega_y$. Notice that, in the corotating frame, $V_{\rm ext}(\mathbf{r})$ does not depend on time. Furthermore $\mu_{\rm loc}(\rho) = g\rho$ is the chemical potential of the uniform gas, where $g = 4\pi\hbar^2 a/M$ is the coupling constant fixed by the s-wave scattering length a and $\mathbf{v}$ is the velocity field in the laboratory frame, expressed in terms of the coordinates in the rotating frame. It satisfies the irrotationality constraint. Equations (1) and (2) can also be applied to a trapped Fermi superfluid, where the expression for $\mu_{\rm loc}(\rho)$ takes, of course, a different form. The stationary solutions in the rotating frame are obtained by imposing the conditions $\partial\rho/\partial t = 0$ and $\partial\mathbf{v}/\partial t = 0$. Let us look for solutions of the form [9]

$$\mathbf{v} = \alpha \nabla(xy) \qquad (3)$$

for the velocity field, where α is a parameter that will be determined later. Choice (3) rules out the description of vortical configurations. Vortices cannot be in any case described by the hydrodynamic equations (1) and (2) since they require the use of more microscopic approaches, such as Gross-Pitaevskii theory for the order parameter, which accounts for the behavior of the system at distances of the order of the healing length [8,10]. Since the critical frequency needed to generate a stable vortex becomes smaller and smaller as the number of atoms increases [11], the solutions discussed in this paper correspond, in general, to metastable configurations.

By substituting expression (3) into Eq. (2), one immediately finds that the resulting equilibrium density is given by the parabolic shape

$$\rho(\mathbf{r}) = \frac{1}{g}\left[\tilde{\mu} - \frac{M}{2}(\tilde{\omega}_x^2 x^2 + \tilde{\omega}_y^2 y^2 + \omega_z^2 z^2)\right] \qquad (4)$$

also in the presence of the rotation. Of course Eq. (4) defines the density only in the region where $\rho > 0$. Elsewhere one should put $\rho = 0$. The new distribution is characterized by the effective oscillator frequencies

$$\tilde{\omega}_x^2 = \omega_x^2 + \alpha^2 - 2\alpha\Omega\,, \qquad (5)$$

$$\tilde{\omega}_y^2 = \omega_y^2 + \alpha^2 + 2\alpha\Omega\,, \qquad (6)$$

which fix the average square radii of the atomic cloud through the relationships

$$\tilde{\omega}_x^2\langle x^2\rangle = \tilde{\omega}_y^2\langle y^2\rangle = \omega_z^2\langle z^2\rangle = \frac{2\tilde{\mu}}{7M}, \quad (7)$$

where the quantity

$$\tilde{\mu} = \frac{\hbar\tilde{\omega}_{ho}}{2}\left(\frac{15Na}{\tilde{a}_{ho}}\right)^{2/5} \quad (8)$$

is the chemical potential in the rotating frame and ensures the proper normalization of the density (4). In Eq. (8) we have defined $\tilde{\omega}_{ho} = (\tilde{\omega}_x\tilde{\omega}_y\omega_z)^{1/3}$ and $\tilde{a}_{ho} = \sqrt{\hbar/M\tilde{\omega}_{ho}}$. The applicability of the Thomas-Fermi approximation, and hence of the hydrodynamic equations (1) and (2), requires that the parameter $15Na/\tilde{a}_{ho}$ be much larger than unity. The rotation of the trap, providing a value of α different from zero, has the consequence of modifying the shape of the density profile, through the change of the effective frequencies $\tilde{\omega}_x$ and $\tilde{\omega}_y$. For certain values of Ω this effect can destabilize the system. Physically one should impose the conditions $\tilde{\omega}_x^2 > 0$, $\tilde{\omega}_y^2 > 0$ to ensure the normalizability of the density.

The equation of continuity (1), which at equilibrium takes the form $(\mathbf{v} - \mathbf{\Omega} \times \mathbf{r}) \cdot \nabla\rho(\mathbf{r}) = 0$, yields the following expression for α:

$$\alpha = -\Omega\left(\frac{\tilde{\omega}_x^2 - \tilde{\omega}_y^2}{\tilde{\omega}_x^2 + \tilde{\omega}_y^2}\right) \quad (9)$$

in terms of Ω and of the effective frequencies $\tilde{\omega}_x, \tilde{\omega}_y$. From (9) and (7), one finds that the expectation value of the angular momentum,

$$\langle L_z\rangle = M\int(\mathbf{r}\times\mathbf{v})_z n(\mathbf{r})\,d\mathbf{r} \equiv \Omega\Theta, \quad (10)$$

is always fixed by the irrotational value $\Theta = NM(\langle x^2 - y^2\rangle)^2/\langle x^2 + y^2\rangle$ of the moment of inertia [12]. In terms of the effective frequencies $\tilde{\omega}_x$ and $\tilde{\omega}_y$ the ratio between Θ and the classical rigid value $\Theta_{rig} = NM\langle x^2 + y^2\rangle$ takes the simple expression

$$\frac{\Theta}{\Theta_{rig}} = \left(\frac{\tilde{\omega}_x^2 - \tilde{\omega}_y^2}{\tilde{\omega}_x^2 + \tilde{\omega}_y^2}\right)^2. \quad (11)$$

Notice that both Θ and Θ_{rig} depend on the value of Ω since the square radii $\langle x^2\rangle$ and $\langle y^2\rangle$ are modified by the rotation.

Another useful quantity is the release energy $E_{rel} = E_{kin} + E_{int}$ giving the energy of the system after switching off the confining trap. This quantity can be extracted from time of flight measurements on the expanding cloud. In nonrotating condensates it coincides with the interaction energy if one works in the Thomas-Fermi regime. In the presence of the rotation the kinetic energy $E_{kin} = M\int d\mathbf{r}\, n(\mathbf{r})v^2/2$ cannot instead be neglected. By using the virial identity [8] $2E_{kin} - 2E_{ho} + 3E_{int} = 0$, where E_{ho} is the expectation value of the oscillator potential, and noting that $E_{int} = (2/7)N\tilde{\mu}$, one finds the result

$$\frac{E_{rel}}{N} = \frac{\tilde{\mu}}{7}\left(\frac{\omega_x^2}{\tilde{\omega}_x^2} + \frac{\omega_y^2}{\tilde{\omega}_y^2}\right). \quad (12)$$

For the total energy $E = E_{kin} + E_{ho} + E_{int} - \Omega L_z$, calculated in the rotating frame, one instead finds the result $E = (5/7)N\tilde{\mu}$.

Let us now discuss the explicit behavior of the stationary solutions of the hydrodynamic equations (1) and (2). By inserting expressions (5) and (6) into Eq. (9) one finds the following third order equation for α [13]:

$$2\alpha^3 + \alpha(\omega_x^2 + \omega_y^2 - 4\Omega^2) + \Omega(\omega_x^2 - \omega_y^2) = 0. \quad (13)$$

Depending on the value of Ω and of the deformation

$$\epsilon = \frac{\omega_x^2 - \omega_y^2}{\omega_x^2 + \omega_y^2} \quad (14)$$

of the trap ($\epsilon > 0$), one can find either 1 or 3 real solutions, derivable in analytic form. As already anticipated, the physical solutions should satisfy the additional requirements $\tilde{\omega}_x^2 > 0$ and $\tilde{\omega}_y^2 > 0$, which ensure the normalizability of the density and rule out some of the solutions of (13). The resulting phase diagram is reported in Fig. 1 where, in the plane Ω-ϵ, we show explicitly the regions characterized by 0, 1, 2, and 3 solutions. The solid curve, given by

$$\frac{\epsilon^2\Omega^2}{\omega_x^2 + \omega_y^2} + \frac{2}{27}\left(1 - 4\frac{\Omega^2}{\omega_x^2 + \omega_y^2}\right)^3 = 0, \quad (15)$$

divides the plane into two parts: On the left-hand side, Eq. (13) admits only one solution; on the right-hand side it has three solutions. The dotted lines are the curves $\Omega = \omega_y = \omega_x\sqrt{(1-\epsilon)/(1+\epsilon)}$ and $\Omega = \omega_x$. If $\epsilon < 0.2$, one can find (see Fig. 1) 3 stationary solutions, by properly choosing the value of Ω [14]. It is worth noticing that the phase diagram in Fig. 1 differs from the one derivable in the noninteracting Bose gas confined by the same harmonic trap. In this case the density profile in the rotating frame has the Gaussian shape $\rho(\mathbf{r}) = N(M\tilde{\omega}_{ho}/\pi\hbar)^{3/2} \times \exp[-M(\tilde{\omega}_x x^2 + \tilde{\omega}_y y^2 + \omega_z z^2)/\hbar]$. The renormalized

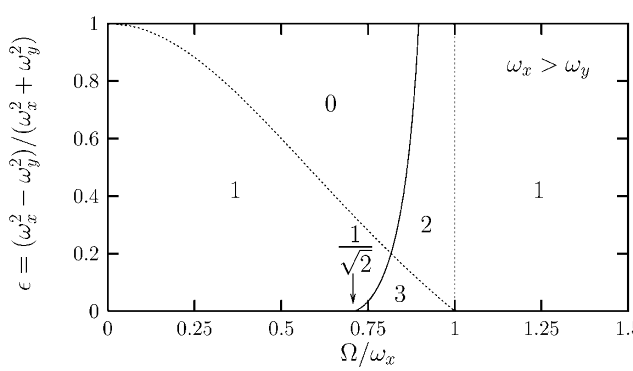

FIG. 1. Phase diagram representing the stationary solutions of Eq. (13) (see text). The dotted lines are the curves $\Omega = \omega_y$ and $\Omega = \omega_x$. The solid line is given by Eq. (15).

frequencies still obey Eqs. (5) and (6), but the relationship for α takes the different form $\alpha = -\Omega(\tilde{\omega}_x - \tilde{\omega}_y)/(\tilde{\omega}_x + \tilde{\omega}_y)$. In the noninteracting case, one finds that only one stationary solution is available for $\Omega < \omega_y$ and $\Omega > \omega_x$, while no solution exists in the interval $\omega_y < \Omega < \omega_x$.

In Figs. 2 and 3 we show the stationary solutions of Eq. (13) for α in two interesting cases: $\epsilon = 0.1$, where we predict the occurrence of a window with 3 stationary solutions, and $\epsilon = 0.5$, where one has a maximum of 2 stationary solutions satisfying the normalizability conditions $\tilde{\omega}_x^2 > 0$ and $\tilde{\omega}_y^2 > 0$. The dash-dotted lines correspond to the stationary solution of the non interacting gas. In both Figs. 2 and 3, one identifies two branches, hereafter called normal and overcritical branches.

(i) *Normal branch.*—This branch starts at $\Omega = 0$. The linear dependence at small Ω is given by $\alpha = -\Omega\epsilon$. By increasing Ω the square radius $\langle y^2 \rangle$ increases and eventually diverges at $\Omega = \omega_y$, where $\tilde{\omega}_y \to 0$ and the branch has its end [15]. Also the angular momentum and the release energy diverge at $\Omega = \omega_y$. Notice that when $\tilde{\omega}_y \to 0$ the moment of inertia takes the rigid value since $\langle x^2 \rangle \ll \langle y^2 \rangle$ [see Eq. (11)]. First experimental studies of the deformed configurations induced by the rotation of the trap have been recently reported in [16].

(ii) *Overcritical branch.*—This branch starts at $\Omega = +\infty$, where α behaves like $\alpha = (\omega_x^2 - \omega_y^2)/4\Omega$. It is worth noticing that in this limit both $\tilde{\omega}_x^2$ and $\tilde{\omega}_y^2$ approach the value $(\omega_x^2 + \omega_y^2)/2$ and therefore the shape of the density profile becomes symmetric despite the asymmetry of the confining trap. In the same limit the angular momentum tends to zero while the release energy approaches the finite value $E_{\rm rel} = (2/7)\tilde{\mu}_\infty$, where $\tilde{\mu}_\infty$ is the chemical potential (8) with $\tilde{\omega}_x^2 = \tilde{\omega}_y^2 = (\omega_x^2 + \omega_y^2)/2$. In the overcritical branch the deformation of the cloud takes a sign opposite to the one of the trap. This branch exhibits a backbending at a value of Ω which is smaller than ω_x, but can be higher or smaller than ω_y, depending on whether the value of ϵ is larger or smaller than 0.2 (see Figs. 2 and 3). In both cases this branch ends, after the backbending, at the value $\Omega = \omega_x$, where $\tilde{\omega}_x \to 0$ and $\langle x^2 \rangle$, $\langle L_z \rangle$, and $E_{\rm rel}$ diverge.

It is also useful to discuss the instructive case $\epsilon \to 0$ corresponding to symmetric trapping in the x-y plane ($\omega_x = \omega_y$). In this case, one finds a solution with $\alpha = 0$ for $\Omega < \omega_x/\sqrt{2}$. For higher frequencies, three solutions appear: the first one still corresponds to a nonrotating configuration ($\alpha = 0$), while two solutions, given by $\alpha = \pm\sqrt{2\Omega^2 - \omega_x^2}$, correspond to rotating deformed configurations. The existence of these two solutions, which break the original symmetry of the Hamiltonian, is the consequence of the fact that the $L_z = 2$ quadrupole mode is energetically unstable for $\Omega \geq \omega_x/\sqrt{2}$ [7,17]. This transition is caused by two-body interactions and is absent in the noninteracting Bose gas. It is the analog of the bifurcation from the axisymmetric Maclaurin to the triaxial Jacobi ellipsoids for rotating classical fluids [18]. With respect to the classical problem of rotating masses our systems are, however, characterized by repulsive two-body forces, the confinement being ensured by the external harmonic force. Furthermore they are characterized by the constraint of irrotationality due to superfluidity. When the deformation of the trap is slightly different from zero the two solutions are no longer degenerate, the one with $\alpha < 0$ having the lowest energy. Even small values of ϵ can affect the solutions near the bifurcation point in a significant way giving rise to important deformations. For example, by using the values $\epsilon = 0.05$ and $\Omega = 0.65\omega_x$, we find that the solution of Eq. (13) corresponds to a condensate with the aspect ratio $R_y/R_x = 1.4$.

The existence of stationary solutions in the rotating frame raises the important question of stability. Actually, one should distinguish between energetic and dynamical instability. The former corresponds to the absence of thermodynamic equilibrium, and its signature, at zero temperature, is given by the existence of excitations with negative energy. The latter is instead associated with the decay of the initial configuration due to interaction effects and is in general revealed by the appearance of excitations with complex energy.

Let us first discuss the stability with respect to the center of mass motion. In the presence of harmonic trapping the

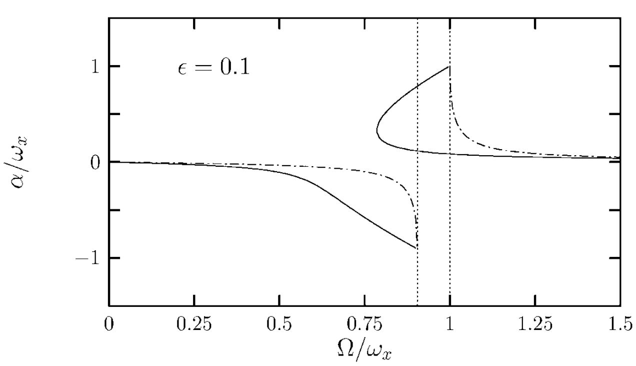

FIG. 2. Stationary solutions of Eq. (13) (solid lines) as a function of Ω, for $\epsilon = 0.1$. The dash-dotted curves are the stationary solutions of the noninteracting Bose gas. The dotted straight lines correspond to $\Omega = \omega_y$ and $\Omega = \omega_x$.

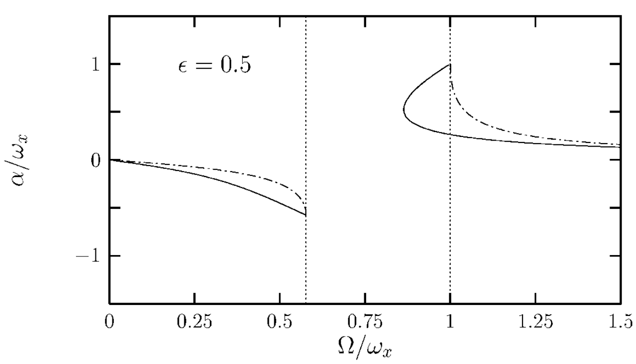

FIG. 3. The same as Fig. 2, for $\epsilon = 0.5$.

corresponding equations of motion, in the rotating frame, take the classical form (rotating Blackburn's pendulum [1]) and are not affected by the interatomic forces. Their solutions obey the dispersion law

$$\omega^2 = \frac{1}{2}\left[\omega_x^2 + \omega_y^2 + 2\Omega^2 \pm \sqrt{(\omega_x^2 - \omega_y^2)^2 + 8\Omega^2(\omega_x^2 + \omega_y^2)}\right],$$

and are dynamically stable ($\omega^2 > 0$) for $\Omega < \omega_y$ and $\Omega > \omega_x$. So the requirement that the dipole oscillation be dynamically stable excludes the region between the dotted lines in Figs. 1–3. Notice that this is the same region where the Schrödinger equation for the noninteracting Bose gas has no stationary solutions in the rotating frame.

We have further explored the conditions of stability by studying the quadrupole oscillations of the condensate around the equilibrium configuration in the rotating frame. The calculation is derivable by linearizing the equations of motion (1) and (2), with the choice

$$\delta\rho(\mathbf{r},t) = a_0 + a_x x^2 + a_y y^2 + a_z z^2 + a_{xy}xy\,, \quad (16)$$

$$\delta\mathbf{v}(\mathbf{r},t) = \nabla(\alpha_x x^2 + \alpha_y y^2 + \alpha_z z^2 + \alpha_{xy}xy)\,, \quad (17)$$

for the fluctuations of the density and of the velocity field, where the coefficients a_i and α_i depend on time. The results of the analysis show that the window of dynamical instability for the quadrupole oscillations is different from the one of the dipole. In particular we find that not only the normal branch but also the overcritical branch is dynamically stable, except in the region with $d\alpha/d\Omega > 0$, where one of the quadrupole frequencies becomes purely imaginary ($\omega^2 < 0$). It is remarkable that one finds stationary solutions of the equations of motion which are stable with respect to internal (quadrupole) shape oscillations also in the window $\omega_y < \Omega < \omega_x$, where the motion of the center of mass is dynamically unstable. This feature is a nontrivial consequence of two-body interactions and seems to be confirmed by first experimental investigations [19]. We have also investigated the stability of the quadrupole excitations in the limiting case $\epsilon = 0$. In this case the upper and lower branches $\alpha = \pm\sqrt{2\Omega^2 - \omega_x^2}$ give rise to a vanishing value for one of the quadrupole frequencies, the others being always real. This vanishing solution corresponds to the rotation of the system in the x-y plane and reflects the rotational symmetry of the Hamiltonian.

At a very low temperature the dynamically stable solutions discussed above are expected to survive, at least for useful time intervals, also in conditions of energetic instability. When collisions are rare and dissipative processes are negligible, these configurations can be destabilized only by nonlinear processes associated with the spontaneous creation of quasiparticles.

Briefly, let us finally discuss the experimental possibility of realizing the rotations described in this Letter. The normal branch could be, in principle, generated by an adiabatic increase of the angular velocity, starting from a cold condensate. The overcritical branch could be instead reached, at least for large values of Ω, by adiabatically switching on a small deformation in the confining potential, rotating at fixed angular velocity [20].

Fruitful discussions with E. Cornell, J. Dalibard, L. Pitaevskii, G. Shlyapnikov, and S. Vitale are acknowledged. This work was supported by the Ministero della Ricerca Scientifica e Tecnologica (MURST).

[1] H. Lamb, *Dynamics* (Cambridge University Press, Cambridge, U.K., 1923), 2nd ed., Sec. 33, Chap. IV.
[2] G. Genta, *Vibration of Structures and Machines* (Springer-Verlag, New York, 1999), 3rd ed.
[3] R. J. Donnelly, *Quantized Vortices in Helium II* (Cambridge University Press, Cambridge, U.K., 1995).
[4] M. R. Matthews *et al.,* Phys. Rev. Lett. **83**, 2498 (1999).
[5] K. W. Madison *et al.,* Phys. Rev. Lett. **84**, 806 (2000).
[6] O. M. Maragò *et al.,* Phys. Rev. Lett. **84**, 2056 (2000).
[7] S. Stringari, Phys. Rev. Lett. **77**, 2360 (1996).
[8] F. Dalfovo *et al.,* Rev. Mod. Phys. **71**, 463 (1999).
[9] This choice, which is associated with a quadrupolar shape of the equilibrium density [see Eq. (4)], corresponds to one of the possible stationary solutions of the equations of motion.
[10] L. P. Pitaevskii, Sov. Phys. JETP **13**, 451 (1961); E. P. Gross, Nuovo Cimento **20**, 454 (1961).
[11] F. Dalfovo and S. Stringari, Phys. Rev. A **53**, 2477 (1996); E. Lundh *et al.,* Phys. Rev. A **55**, 2126 (1997).
[12] J. J. Garcia-Ripoll and V. M. Perez-Garcia, cond-mat/0003451; F. Zambelli and S. Stringari, cond-mat/0004325.
[13] A. Recati, diploma thesis, Università di Trento, 1999. Notice that this equation is independent of the equation of state $\mu_{\rm loc}(\rho)$ entering Eq. (2) and holds, in particular, also for a trapped Fermi superfluid.
[14] The value $\epsilon = 0.2$ corresponds to the intersection between Eq. (15) and the curve $\Omega = \omega_y$.
[15] Near the end point the conditions of applicability of the Thomas-Fermi approximation are no longer valid and the solution of the problem should be obtained starting from the Gross-Pitaevskii equation.
[16] J. Arlt *et al.,* J. Phys. B **32**, 5861 (1999).
[17] F. Dalfovo *et al.,* Phys. Rev. A **56**, 3840 (1997).
[18] S. Chandrasekhar, *Ellipsoidal Figures at Equilibrium* (Yale University Press, New Haven, CT, 1969); P. G. Drazin, *Nonlinear Systems* (Cambridge University Press, Cambridge, U.K., 1994).
[19] J. Dalibard (private communication).
[20] Under these conditions the wave function associated with the overcritical branch is in fact very close to the one with the nonrotating configuration.